Forest Ecology and Management 543 (2023) 121142

Contents lists available at ScienceDirect

Forest Ecology and Management

journal homepage: www.elsevier.com/locate/foreco

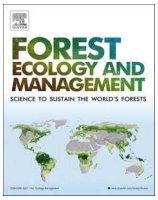

Quantifying the effectiveness of shaded fuel breaks from ground-based, aerial, and spaceborne observations

Janine A. Baijnath-Rodino [a,*], Alexandre Martinez [a,b], Robert A. York [c], Efi Foufoula-Georgiou [a,d], Amir AghaKouchak [a], Tirtha Banerjee [a]

[a] University of California Irvine, Department of Civil and Environmental Engineering, Interdisciplinary Science and Engineering Building, Irvine, CA 92697, United States
[b] Department of Exposure Modeling, Risk Management Solutions, Inc. Newark California, 94560, United States
[c] Department of Environmental Science, Policy, and Management, University of California, Berkeley, Georgetown 94720, United States
[d] Department of Earth Systems Science, University of California-Irvine, Irvine, CA, United States

ARTICLE INFO

Keywords:
Multispectral analysis
Remote Controlled Aerial Vehicles
Fuel break
Wildfires
Burn severity

ABSTRACT

Shaded fuel breaks are treatments that aim to mitigate wildfires by establishing linearly aligned locations where wildfire suppression efforts can be more effective at stopping wildfires. Despite the potential of fuel breaks to alter fire behavior, there have been limited quantitative assessments of their effectiveness following exposure to wildfires. In addition, wildfires often occur in complex terrains that are difficult to access with ground vehicles and sensors, posing challenges for data acquisition. However, the use of Remote-controlled Aerial Vehicles (RAVs), such as drones, is becoming increasingly popular as a viable means of conducting high-resolution observations in areas of interest. This study presents the results from a unique opportunity to utilize three distinct observation scale platforms (in-situ, aerial, and spaceborne) to investigate the burn severity impacts across a prior shaded fuel break that serendipitously encountered the 2020 Creek Fire in the Sierra Nevada forests of California, USA. To provide a direct measure of fire severity, ground-based measurements determined the percentage crown volume (PCV) of scorch and char as a function of distance from the fuel break edge. Along five transects of the fuel break, we also utilized visible bands from drone imagery and digital photogrammetry, to generate georeferenced orthophotos and quantify vegetation health using the Green Leaf Index (GLI). We also quantified burn severity by computing the Delta Normalized Burn Ratio (dNBR) and vegetation health using the Normalized Difference Vegetation Index (NDVI) from Sentinel 2 spaceborne observations. Our results indicate that within the fuel break, the PCV of char is 2 × less than it was outside of it (with PCV char declining at a rate of 2% per 3 m into the fuel break). Burn severity is 5 × less, and vegetation health is approximately 3 × greater within the fuel break compared to directly outside. Furthermore, postfire vegetation health was only 1 × less within the fuel break compared to the pre fire condition, whereas it was 5 × less in the surrounding region. The results confirm that the fuel break altered the fire behavior, reducing the fire intensity, thereby proving effective at reducing fire burn severity and preserving vegetation health within the fuel break.

1. Introduction

Fuel breaks are a natural (e.g., rocky outcrops) or artificial (e.g., fuel treatments) change in fuel characteristic that helps to regulate fire behavior (National Wildfire Coordinating Group: Accessed January, 2022). Fuel treatments, such as mastication, thinning, chipping, and prescribed burning are human-imposed ways to help mitigate and control fires, while maintaining ecosystem health. Fuel treatments produce discontinuity of surface, ladder, and crown fuels, thereby reducing the risk of intense crown fires (VanWagner, 1977; Agee et al., 2000; Scott and Reinhardt, 2001; Vaillant et al., 2009; Banerjee, 2020).

Types of fuel reduction treatments include mechanical methods, prescribed burns, and a combination of both. When done specifically for the objective of reducing fire severity, mechanical treatments reduce tree density and canopy bulk density, and increase canopy base height, thereby reducing horizontal and vertical continuity between surface and crown fuels (Vaillant et al., 2009; Banerjee, 2020; Keyes and O'Hara, 2002; Stephens et al., 2009). Prescribed fire treatments reduce surface

* Corresponding author.
E-mail address: jbaijnat@uci.edu (J.A. Baijnath-Rodino).

https://doi.org/10.1016/j.foreco.2023.121142
Received 27 February 2023; Received in revised form 22 May 2023; Accepted 24 May 2023

and ladder fuels but do not necessarily reduce canopy fuels given their typically low intensities (Vaillant et al., 2009; Stephens et al., 2009; Knapp et al., 2005; Keifer et al., 2006; Stephens and Moghaddas, 2005; Agee and Lolley, 2006). The combination of mechanical treatments followed by prescribed burns has been shown to be particularly effective at reducing burn severity (Stephens et al., 2009; Stephens and Moghaddas, 2005; van Wagtendonk and Erman, 1996; Peterson et al., 2003; Ritchie et al., 2007). These fuel treatments are ideally effective for reducing fire intensity (reduce flame length) and can be strategically placed either to protect high value areas or to create opportunities for fire suppression to stop wildfires (Agee et al., 2000; Banerjee, 2020; Ritchie et al., 2007; Pollet and Omi, 2002; Martinson and Omi, 2003; Finney et al., 2005; Moghaddas and Craggs, 2007; Banerjee et al., 2020).

Despite the scientific consensus on the impact of fuel reduction and removal in altering fire behavior, there are limited quantitative studies that have assessed this assertion specifically in treated areas subsequently exposed to wildfire (Hudak et al., 2011). Quantitative assessments using process-based modeling was applied in a study (Banerjee, 2020) to simulate different degrees of thinning in order to determine the various levels of response that thinning would have on wildland fire behavior. The study found that thinning can generally lead to reduced fire intensity due to lower fuel availability. However, a low degree of thinning, below certain thresholds, can lead to strong wind and light entrainment inside a forest canopy, thereby potentially offsetting the effects of fuel reduction and increasing fire intensity and rate of spread. Thus, the degree of thinning thresholds is a functions of micrometeorological features of the canopy environment (Banerjee, 2020). Although the capabilities of fuel treatments are predominantly shown from model simulations, empirical testing and validation is lacking, and these can only be accomplished by opportunistic collection of data when wildfires serendipitously encounter fuel treatments (Hudak et al., 2011).

The effectiveness of a fuel break can be quantified through ground-based, aerial, and spaceborne observations. Only a few empirical studies have documented fuel treatments that have subsequently encountered wildfires over different forested fire regimes and ecosystems across the United States from the 1960 s to the early 1990 s (Cumming, 1964; Van Wagner, 1968; Wagle and Eakle, 1979; Omi and Kalabokidis, 1991; Syphard et al., 2011), and from 1980 s to the early 2000 s (Syphard et al., 2011). These studies compared the effectiveness of fuel treatments by assessing the postburn severity after a wildfire moved over the treated areas. These investigations were predominantly conducted using ground-based observations for determining unburned, light, spotty moderate, and severe burn severity. In-situ measurements can provide high-resolution monitoring of burn severity at the individual tree scale by visually assessing fire-related damage to tree crowns. However, ground-based measurements can be laborious when observing burn severity over many acres, and with burns occurring in complex topography, it is often difficult to gain ground access to the study site in order to conduct surveys.

The advent and improvement of aerial and spaceborne remote sensing systems prove useful for observing forestry parameters, such as fuels, vegetation and fire behavior with different resolutions (spatial, temporal, and spectral) for various forest management purposes (economic, conservation, restoration) (Dainelli et al., 2021). Remote controlled aerial vehicles (drones) are advantageous for precision forestry monitoring due to their real-time observations, relatively lower operational cost and higher spatial and temporal resolution compared to satellite remote sensing. Drones also facilitate and improve field data collection by customizing specific practical forestry research objectives (Dainelli et al., 2021; Chianucci et al., 2016; Surovỳ and Kuželka, 2019). Drone information can be combined with photogrammetric techniques to build detailed three-dimensional models of the environment (Bright et al., 2016; Shin et al., 2018; Moran et al., 2019). Some disadvantages of drone monitoring within forested regions include the challenge of maneuvering the drone through dense forest canopy and avoiding obstacles. If ash is on the ground, the powerful rotors of the drone can produce ash plumes, obscuring the sensor. In general, drones are also limited by weather conditions, battery operations, payload weight, flight airspace restrictions and regulations. Furthermore, large data processing capabilities are required for post-processing of images that require sophisticated machine learning systems and software, resulting in substantial computational needs (Syphard et al., 2011; Shin et al., 2018; Moran et al., 2019; Gómez et al., 2019).

Spaceborne observations (satellites) data can be assimilated into informational products that lend a cost-effective way of mapping wildfire threats to people and the environment, allowing the prioritization of response measures (Richard et al., 2020), and providing consistent temporal coverage. In contrast to aerial observations, satellites are able to avoid certain imaging geometric problems (foreshortening, layover, shadowing). This is due to having a relatively narrower range of incidence angles, generated from being at an altitude of several hundred kilometers higher than aerial observation platforms (Resource, 2022), though this may not apply to all sensors. However, satellites are not always ideally suited for regional or local scale forestry objectives because satellite observations are limited by overcast cloud conditions that can attenuate electromagnetic waves, resulting in data loss and degradation depending on the observation sensor (Dainelli et al., 2021; Guimarães et al., 2020). Each observation method, while having both pros and cons, can provide useful information about forestry management techniques, when combined.

In this study, we present a unique case wherein we empirically evaluate the effectiveness of a fuel treatment that was subsequently exposed to the 2020 Creek Fire in California, using ground-based, aerial, and spaceborne observations. We monitor the postburn vegetation health of the fuel-treated and untreated region to (1) quantify how effective the fuel treatment was at preserving vegetation health during an intense wildfire, and (2) provide a comparison of the three observation methods in quantifying burn severity and ecological health.

2. Data and methods

2.1. Region of interest

This case study investigates the change in burn severity following a wildfire as it burned across a shaded fuel break that was created one year prior to the Creek Fire in September 2020. The California Department of Forestry and Fire Protection (CAL FIRE) documented that the Creek Fire was located on both sides of the San Joaquin River near Mammoth Pool, Shaver Lake, Big Creek and Huntington Lake at an approximate coordinate of 37.19147 N, 119.261175 W in Fresno, California. The fire burnt over 1,200 km^2. The region of interest, which comprised the fuel treatment area, was located within the wildfire footprint near Shaver Lake at a 1524 m elevation (Fig. 1). The fuel break had been created by thinning the fuels to approximately 23 m^2/ha residual basal area. Harvested trees that were large enough to produce sawlogs, were skidded to nearby landings. Trees not large enough to have sawlogs were cut and piled throughout the fuel break. Finally, mastication of shrubs and small trees was conducted, resulting in a relatively low density and low fuel load structure. This structure is typical of shaded fuel breaks where the objective is to provide a linear feature on the landscape that provides personnel with an increased opportunity to halt a wildfire's advancement. The fuel break region analyzed was approximately 400 m in length and 120 m wide.

2.2. In-situ observations

We quantified the postburn severity of the Creek Fire across the fuel break by collecting ground-based observations and computing two burn severity metrics. First, the percent crown volume (PCV) damage was measured as the total amount of the crown that was killed by the fire. The PCV was determined by observing the crown and giving an ocular estimate of the percent of the crown that was scorched (brown color) or

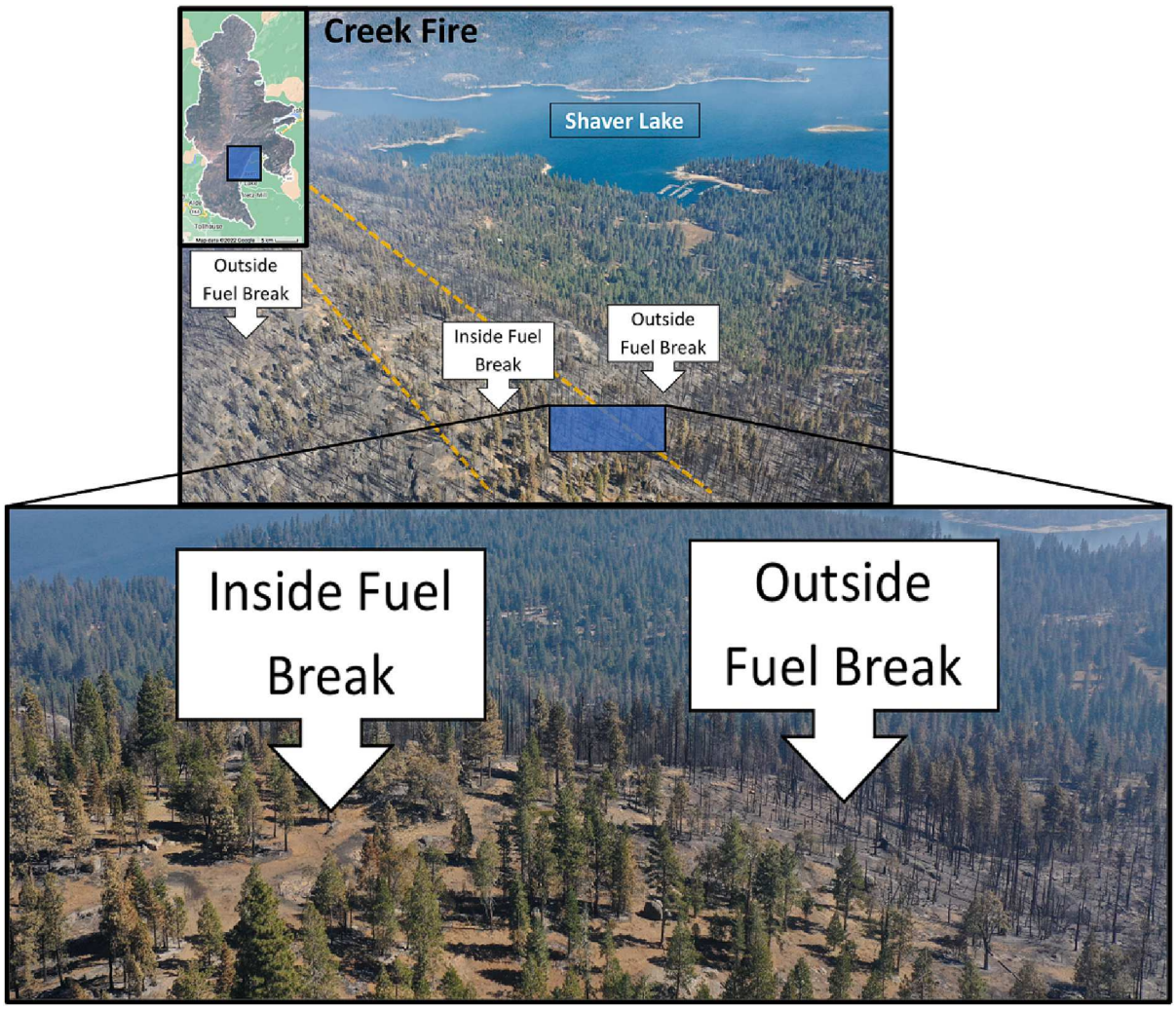

Fig. 1. Perimeter of the overall Creek Fire (top left) and the zoomed in visible drone images of the study region, showing the delineation of the inside and outside regions of the fuel break.

charred (black), to the nearest 5%. The PCV included an estimate of the combination of both scorch (from heating of needles) and char (from fire actively consuming needles in crowns). We analyzed the combined PCV of both scorch and char, as well as individual PCV that was charred and PCV that was scorched. Since fuel treatments function to reduce wildfire related mortality, the specifics of scorched or charred levels are not of great importance, hence why they can be combined. However, it is noted that within the context of a fuel break that functions to allow fire suppression personnel to extinguish a fire, charring and scorching are distinct. This is because an active crown fire that is charring crowns is much less likely to be contained and is also projecting far more embers compared to a surface fire that is causing crown scorch. Therefore, for the purpose of this study we analyzed the combination of PCV (char and scorch) as well as PCV of char, and the PCV of scorch, separately.

The data were collected along five transects from the fuel break line, trying to avoid large rocks or landings. Our team oriented the transects to run perpendicular to the long axis of the fuel break. This was estimated visually. The azimuth (from a set origin point to the end of a 60 m horizontal distance) could vary by no more than 20 degrees, with the entire offset varying no more than 20 m. We used evidence from fuel break treatment (stumps, skid trails, masticated material, and stem density) in order to determine the boundary of the fuel break. Marking the transect origin with a pin flag, we were able to find the azimuth of the transect direction with a compass. Each transect had its own ID (e.g., 1A-OUT, 1A-IN, 1B-IN, 1B-OUT; 2A-OUT, 2A-IN, 2B-IN, 2B-OUT). For example, transect 1A-OUT represents transect one, for which the fire is on the outer front edge of the fuel break, making its way towards the fuel break; 1A-IN is transect one that is within the fuel break and signifies that the fire has now entered the fuel break and is moving to the center of the fuel break; 1B-IN represents the transect for which the fire is within the fuel break but moving out towards the back edge of the fuel break; 1B-OUT represents the transect where the fire has now exited the fuel break and is propagating away from the outer edge of the fuel break. Each of these transects are approximately 60 m in length. This pattern is repeated for transects 0 to 4 (Fig. 2). The average PCV scorch from all transects at increments of approximately three meters was computed to determine the trend in PCV scorch across the fuel break. A similar approach was used to determine the trend in PCV of char.

2.3. Remote sensing observations

Aerial and spaceborne remote sensing were used to observe the vegetation health and burn severity across the fuel break. The aerial drone observations were used to compute the Green Leaf Index (GLI), and the spaceborne satellite observations were used to calculate the delta normalized burn severity (dNBR), as well as the normalized difference vegetation index (NDVI). The drone observations were conducted to determine the postburn vegetation health across the fuel break, using the visible range red, green, and blue (RGB) imagery acquired from the DJI MAVIC PRO. We manually flew and captured RGB

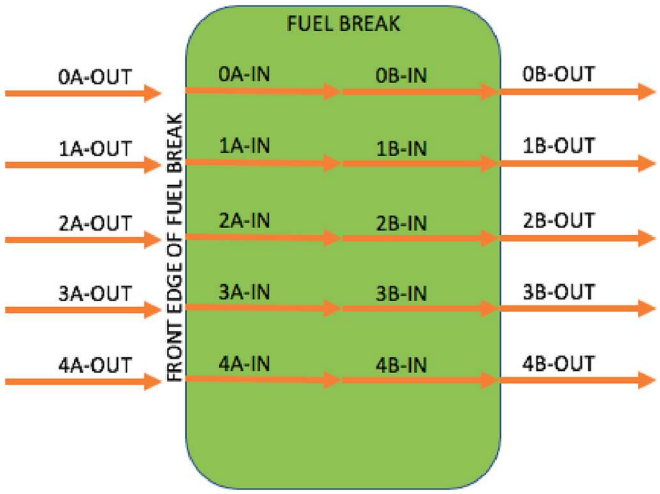

Fig. 2. Schematic of the executed transect paths across the fuel break area (green) to collect ground observations, with each transect having its own ID, spanning 60 m from the edge towards the center of the fuel break (IN) or away from the front edge of the fuel break (OUT).

images with the drone at a height of 120 m, across the width of the fuel break line at five different transects (in and out of the fuel break) at a distance length of 60 m.

From the visible RGB imagery, we created a georeferenced orthophoto, on which our vegetation index could be applied. Since the drone was limited to only observing in the visible part of the electromagnetic spectrum, the presence of living vegetation for postfire was determined by computing (*GLI*), a spectral index that only relies on the visible domain of the electromagnetic spectrum, Eq. (1):

$$GLI = \frac{2\rho_{\lambda_1} - \rho_{\lambda_2} - \rho_{\lambda_3}}{2\rho_{\lambda_1} + \rho_{\lambda_2} + \rho_{\lambda_3}} \quad (1)$$

where ρ_{λ_k} is the spectral reflectance in waveband k and λ_1, λ_2, and λ_3 represent the green, red, and blue bands, respectively (Louhaichi et al., 2001). GLI, is sensitive to the leaf chlorophyll content and is used to detect changes in the chlorophyll content of crops and foliage (Bush et al., 2020). Negative values represent bare soil and non-vegetation, and positive values represent living green leaves and stems (Eng et al., 2019). We acknowledge that several other RGB indices exist for assessing vegetation health, such as the visible atmospherically resistant index (VARI) and the visible atmospherically resistant indices green (VIgreen), but GLI performs better for detecting living vegetation in comparison to the other indices in both urban and forested regions (Eng et al., 2019).

The spaceborne satellite observations were provided by Sentinel 2 (S2) and has a temporal resolution pass of every five days. S2 is used to determine both dNBR and NDVI. The dNBR is calculated by computing the bi-temporal differenced reflectance in the normalized burn ratio (NBR) (Eq. (2)). The NBR estimates the burn severity by using the near infrared (NIR) and shortwave-infrared (SWIR) bands (van Gerrevink and Veraverbeke, 2021), Eq. (3):

$$dNBR = PrefireNBR - PostfireNBR \quad (2)$$

$$NBR = \frac{\rho_{\lambda_4} - \rho_{\lambda_5}}{\rho_{\lambda_4} + \rho_{\lambda_5}} \quad (3)$$

where λ_4 and λ_5 represent the NIR and SWIR bands, respectively. Healthy vegetation, prior to a fire, would have high reflectance in the NIR and a low SWIR response. However, recently burnt vegetation would have a low reflectance in the NIR and a high reflectance in the SWIR (Keeley, 2009; Fassnacht et al., 2021).

In this study, we specify the time period for the PrefireNBR to occur between August 3 to September 3, 2020, and the PostfireNBR to occur between October 3 to November 3, 2020, with data acquisition time repeating every 5 days. The preNBR and postNBR were calculated from the NIR and SWIR (bands 8 and 12) at 10 m and 20 m spatial resolutions, respectively.

Similarly, NDVI was calculated for the prefire dates and the postfire dates, as a function of NIR (band 8) and the red band (band 4) at 10 m spatial resolution for both bands, Eq. (4) (Rouse et al., 1974).

$$NDVI = \frac{\rho_{\lambda_4} - \rho_{\lambda_2}}{\rho_{\lambda_4} + \rho_{\lambda_2}} \quad (4)$$

NDVI is used to determine vegetation health, drought assessment, forest fire risk zones, agricultural yield, and relative estimates of biomass vegetation. High absorption in the red band denotes the high presence of chlorophyll, while high reflection in the NIR represents internal leaf structure (Somvanshi and Kumari, 2020). Subsequently, using the generated orthophoto of the fuel break region, we applied five transect lines of approximately 500 m across the fuel break. The average metric across the five transect lines at a distance of approximately 10 m increments was computed to determine the trend of each metric across the fuel break.

3. Results and discussion

3.1. Ground-based observations

Ground-based observations were conducted to determine the effectiveness of the fuel break in influencing the percent crown damage and percent crown char. Overall, crown damage (as a function of both scorching or charring) was high on both the outside and inside the fuel break, averaging over 80% crown volume damage per tree. However, the difference between the outside and inside of the fuel break was more noticeable for PCV that was charred, compared to that of scorch (Fig. 3). The PCV of char within the fuel break was less than 40% whereas the region outside was doubled, at approximately 80%. This suggests that charring was significantly reduced within the fuel-treated region. The PCV of scorch was observed to increase within the fuel break than on the outside (not shown). This is not surprising as the trees outside of the fuel break had a greater PCV of char, allowing for little to no observed scorch, whereas within the fuel break the PCV of char is reduced, allowing for the less severe scorch signals to become more apparent.

Quantifying the PCV of crown char as a function of distance from the edge of the fuel break, we observe a significant relationship between the

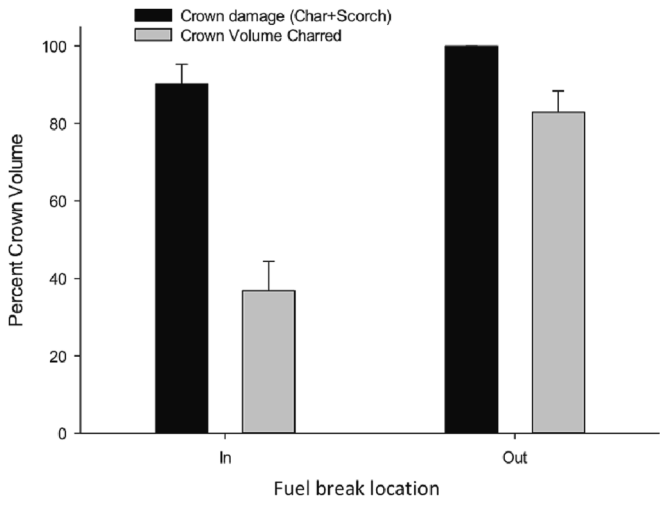

Fig. 3. Percent crown volume from the sum of char and scorch (black bars) and just char (gray bars) of the vegetation within (In) and outside (Out) the fuel break region.

distance from the fuel break edge and crown char (Fig. 4). As the fire entered the fuel break, PCV char declined quickly (p less than 0.001) at a rate of 1.9% per 3 m. As the fire left (or entered from spotting), the PCV char increased significantly, at a rate of 2.1% per 3 m. From ground-based observations, the fuel break did very little to reduce the mortality from the wildfire when considering both char and scorch, but was effective at reducing the PCV of char within the fuel break. Furthermore, the fuel break appeared to also change the behavior of the wildfire. While there may be some effectiveness of strategic shaded fuel breaks for modifying fire behavior, it is important to note that fuel break is not a stand-alone strategy but should be complemented with a combination of fuel treatments (such as prescribed burns) (Agee et al., 2000), in order to produce better effects at stand and landscape scales for reducing large-scale wildfires and high severity burns.

The ground-based observations allow for very high spatial resolution mapping of each individual tree to discern between the charred and scorched burn damages as a function of distance from the fuel break. However, some challenges exist in discerning coloration of tree damage (brown for scorch) or green for unburnt when the presence of ash on the canopy obscures the leaf color. An ideal time to conduct these in-situ measurements is after a rainfall event that quickly follows the wildfire. The rain removes the ashes from the canopy in order to clearly visually observe the canopy color.

3.2. Remote sensing observations

Based on the visible aerial images from the drone observation, a georeferenced orthophoto was created of the postburn region (Fig. 5), indicating a clear delineation of the fuel break region, edge effects, and surrounding unburnt landscape. The average GLI value across the transect of the fuel break was plotted (Fig. 6). The average GLI value within the fuel break is approximately 0.2, whereas the values outside averaged closer to 0, indicating that chlorophyll levels and live vegetation are higher within the fuel break, but only slightly. This increase in GLI is weak and can be fraught with uncertainties due to limitations of the GLI algorithm that only uses the visible part of the electromagnetic spectrum. In addition, high spatial resolution data acquisition from drones could introduce noise, such as shadowing effects, introducing uncertainties in computing GLI.

The aerial observations allowed us to quantify vegetation health using the GLI (RGB) bands at a high spatial resolution, as well as at a relatively large but localized spatial extent. The collection and processing of drone data has the potential to fill the gap between ground-based and satellite observations (Yang et al., 2020) but in this study, the difference in GLI values within and outside the fuel break is not as apparent as the ground-based and satellite observations. However, some limitations from the current study include the lack of multispectral and hyperspectral sensors onboard our drone flight for capturing NIR and SWIR for additional dNBR and NDVI analysis. Mounting thermal, multispectral, and lidar sensors on future drone missions will offer improved high spatial and spectral resolution for obtaining burn severity metrics for monitoring postburn vegetation health and fuel load. Nevertheless, the postprocessing of the RGB images captured by the drone, in this study, allows for additional data acquisition that can generate detailed orthophotos, which can further be implemented into fire behavior models. This can assist in improving the parameterization schemes of digital elevation, topography, fuel load, and fuel type characteristics that can subsequently improve physics-based modeling in order to better understand the influence of potential fuel treatments on fire behavior (Vaillant et al., 2009; Stephens, 1998; Schmidt et al., 2008). Despite the shortcomings of the drone data acquisition for this particular case study, the digital orthophoto generated from the drone RGB data was deemed beneficial because it could be overlaid on the coarser spatial resolution satellite datasets to provide precise georeferenced images of the localized study area.

The effectiveness of the fuel break line was also quantified by determining the dNBR and NDVI using S2. The results show that within the fuel-treated area, the dNBR values (scaled by a factor of 10^3 in this study) indicate areas of unburned classes (values between −100 to 99). Along the edges of the fuel break, the dNBR values increased to low severity burn (100 to 269). The outer, untreated regions have dNBR values corresponding to moderate to high severity burns with values generally ranging between 660 and 1300 (Fig. 7). On average, the dNBR outside of the fuel break was 505 while within the fuel break the dNBR was 85. This suggests that the burn severity was 5 × less within the fuel treated region and is statistically significant at the 99% confidence level

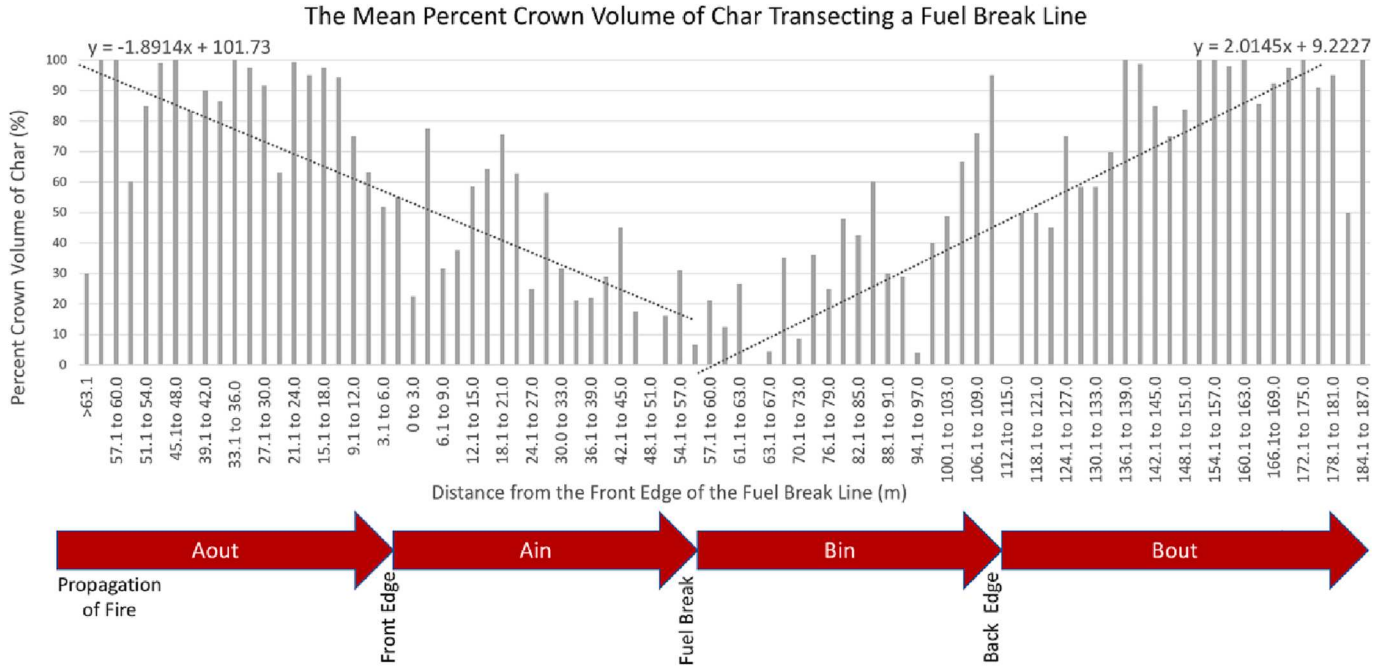

Fig. 4. The relationship between the distance from the fuel break edge with respect to the PCV that was charred, as the fire entered (Aout), propagated through (Ain and Bin) and left (Bout) the fuel break line.

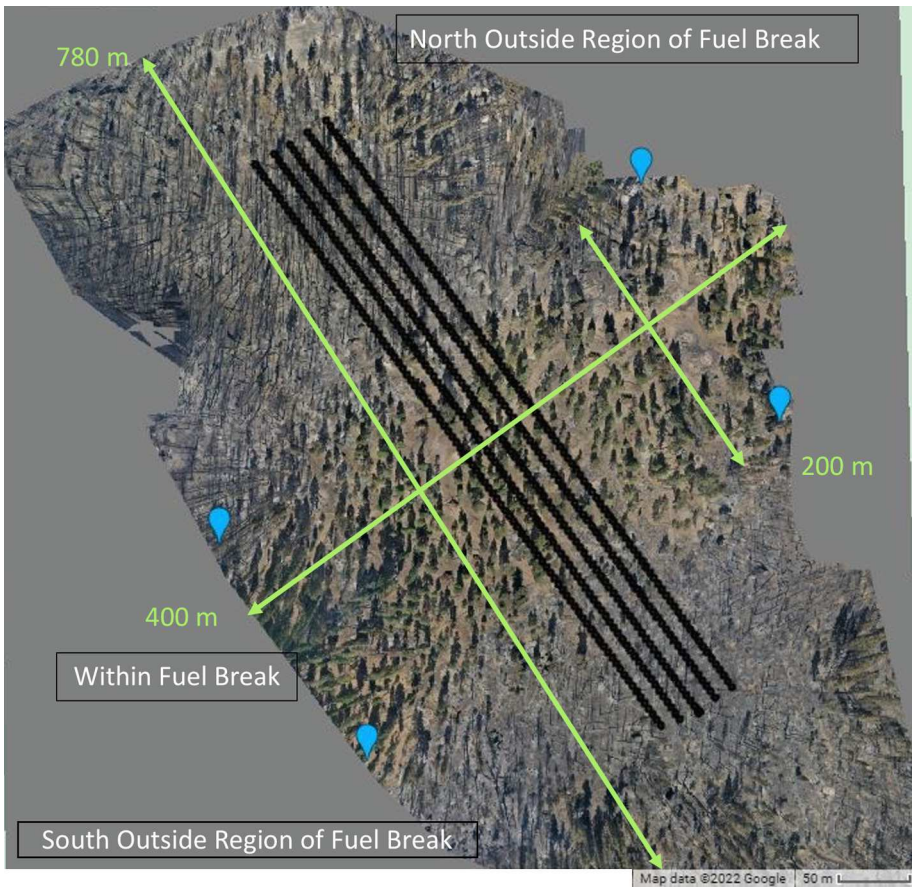

Fig. 5. Digital orthophoto generated from the visible drone imagery, providing an orientation of the postburn landscape, with the demarcation (green) of the length and width of the fuel break region and the surrounding untreated region, the edges of the fuel break (blue) and the five transect lines (black).

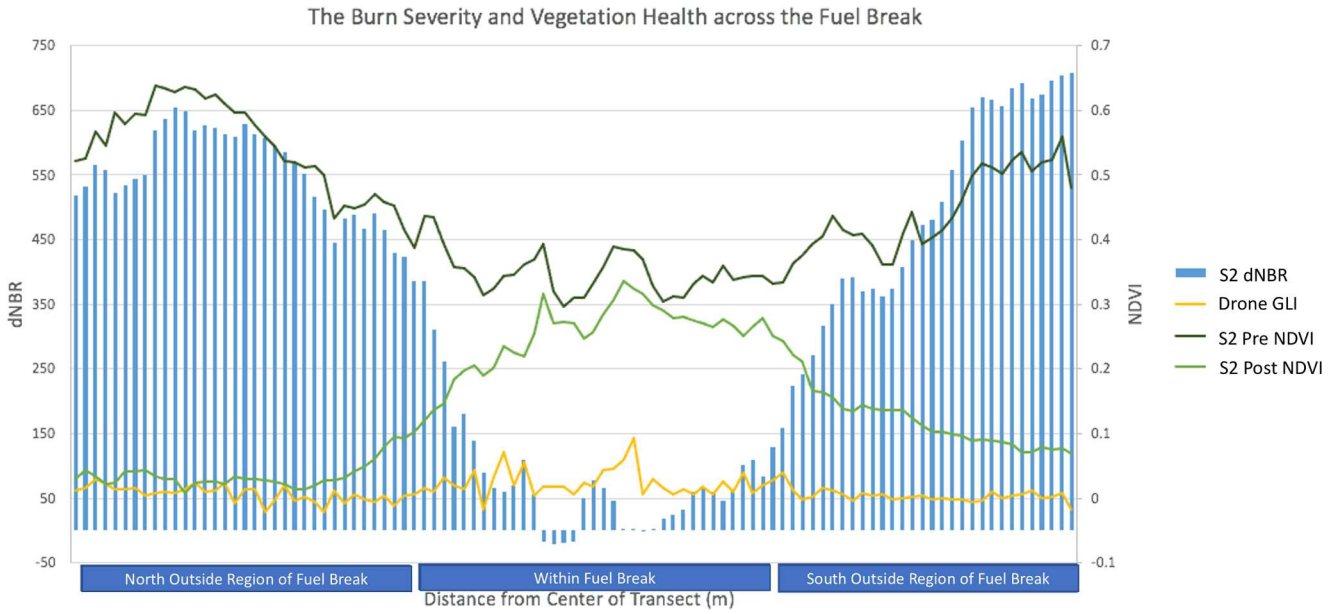

Fig. 6. The burn severity and vegetation health metrics plotted within and outside of the fuel break region for each of the observational sensors: the S2 dNBR (blue bars), prefire NDVI (dark green line), postfire NDVI (light green line); the drone GLI (yellow line).

(Fig. 6).

A low burn severity within the fuel break is also indicative of a healthier postfire vegetation within the fuel break. The average postfire NDVI is 0.24 and 0.09 within and outside the fuel break, respectively. Thus, postfire NDVI within the fuel break is approximately 2.7 × greater than the NDVI outside the fuel break and this increase is statistically significant at the 99% confidence level (Fig. 6). Prefire NDVI shows an opposite trend, with average values within and outside the fuel break of

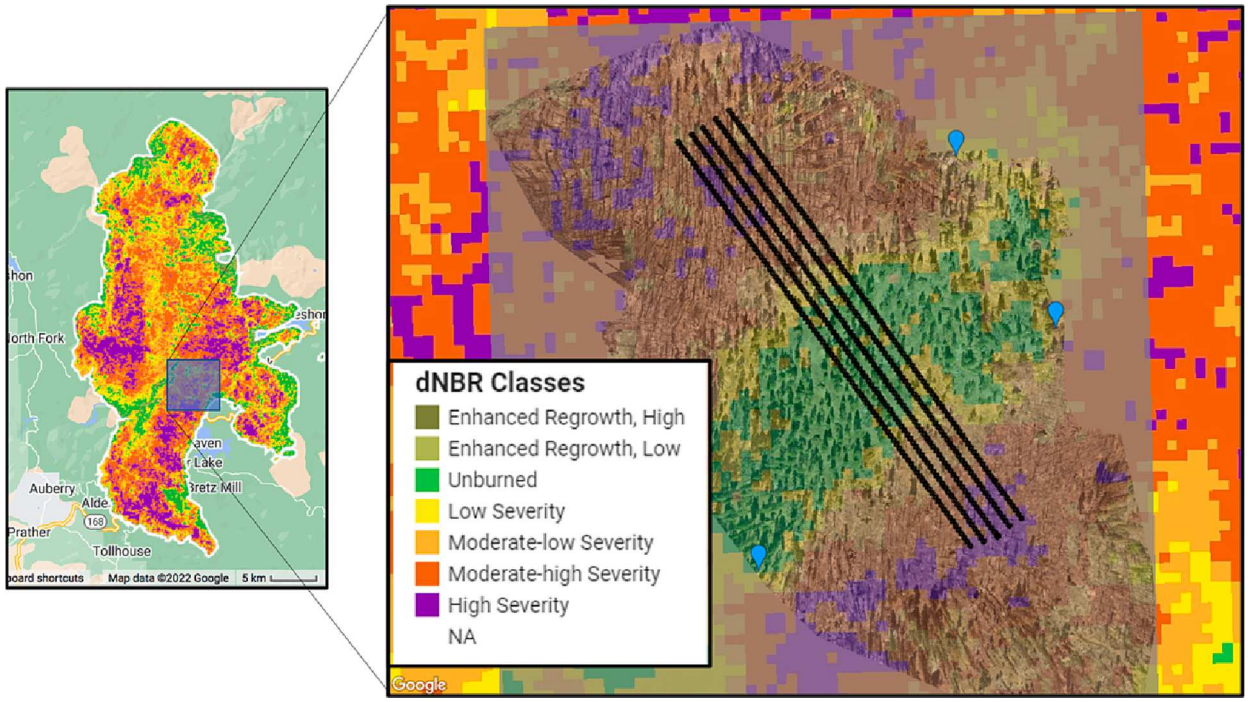

Fig. 7. Map of the dNBR for the overall Creek Fire area (left panel) and the orthophoto of the fuel break region overlaid on the S2 dNBR layer (right panel), with high severity burns (purple) with values of 1300, and unburned areas (green) with values as low as −100. The Creek Fire perimeter shapefile was provided by the Government of California, California State Geoportal (Google Earth Engine, 2022), and Google Earth Engine (Government of California, 2021) was used to generate the burn severity map.

0.35 and 0.47, respectively. The NDVI within the fuel break is approximately 1.4 × lower than the NDVI outside the fuel break and is statistically significant at the 99% confidence level. This is expected, as prior to the Creek Fire, the shaded fuel break would have less dense canopy vegetation compared to its surroundings, thereby, exposing barer soil and ground and reducing the NDVI value. Furthermore, when comparing the average preNDVI (0.5) and postNDVI (0.09) outside of the fuel break, results indicate that the vegetation health was 5 × lower after the fire. However, within the fuel break, the average preNDVI (0.35) and postNDVI (0.25) resulted in only a 1.4 × decrease. Therefore, the NDVI findings suggest that the shaded fuel break was effective at preserving the vegetation health after the Creek Fire and staved off more severe damages. Thus, by quantifying vegetation health and burn severity at the various scales (by in-situ, aerial, and spaceborne observations) it is evident that there is a clear delineation that the vegetation health was preserved within the fuel treatment area of the fuel break line, while the untreated region experienced high severity burns from higher intensity flames.

The satellite S2 observations offered the opportunity to expand our analysis and use additional bands in the NIR and SWIR to be able to quantify burn severity. However, differentiating between different vegetation species can be challenging with, relatively, coarse-resolution satellite observations (Yang et al., 2020). Some additional caution when using satellite observations to quantify dNBR is being aware of detecting external surface-atmospheric features pre and postfire events, such deforestation and other land cover changes that can introduce non-fire related detection features. In addition, cloud and snow shadowing effects, although masked in the pre-processing steps, can sometimes fail, leading to false detection, such as enhanced regrowth (Chu and Guo, 2013). Analyzing pre- and postfire events within a short time period, as carried out in this study, reduces the likelihood of external surface-atmospheric changes that can alter the fire detection.

In this specific case study, we determined that the fuel treatment examined, herein, was effective at reducing the burn severity of trees within the fuel break. However, fuel breaks do not necessarily function effectively on their own. Here we discuss some additional forest management strategies that complement fuel break objectives and present some limitations to fuel break plans. The fuel break we examined was intended to create linear features that promoted lower intensity fires and burn severity at a relatively small spatial scale in comparison to wildfires that generated large-scale effects across the landscape. Although this fuel break was effective, it is suggested that a combination of fuel breaks with surrounding large scale fuel treatments can reduce the size and intensity of wildland fires (Agee, 1996). A study (Syphard et al., 2011) showed that fuel breaks were effective at stopping wildfires in 46% of the fire events examined and was predominantly due to the fact that these fuel breaks allowed for fire fighter accessibility to aid in the fire suppression efforts. In addition, it is also important to consider the strategic placement of fuel break networks, which is site-specific with various objectives, such as for aiding in managing entire landscapes and protecting special features (such as nearby communities and ecosystems at risk (Agee et al., 2000; Omi, 1996). Despite strong opinions for placing fuel breaks near communities where protection is most needed (Syphard et al., 2011), most fuel breaks continue to be located in more remote wildland areas (Syphard et al., 2011; Ingalsbee; Schoennagel et al., 2009). While fuel treatments can help protect people from wildfires, some may not be mutually beneficial to ecosystems with infrequent crown fires (Wilkin et al., 2017). Some short-term studies indicate fuel reduction and treatments can be detrimental to biodiversity and ecosystem function. Furthermore, long-term ecological trajectories and fuel hazard outcomes of fuel treatments are still poorly understood (Wilkin et al., 2017).

4. Conclusions

This study presented a unique opportunity to evaluate the effectiveness of a shaded fuel break following its serendipitous exposure to extreme flames during the 2020 Creek Fire. In addition, observing the postfire fuel break at three distinct observation scales provided a novel approach for empirically quantifying the effectiveness of the fuel break

at preserving vegetation health and reducing burn severity.

We applied three observational techniques and their corresponding methods for quantifying vegetation health and burn severity within and outside of the fuel break. For in-situ measurements, the PCV of scorch and char were determined at the tree-scale level. Aerial measurements were used to quantify the presence of healthy vegetation by computing the GLI, using RGB data from drone-based observations. Spaceborne measurements, obtained from S2, were acquired to quantify burn severity and vegetation health, using the dNBR and NDVI metrics, respectively (see the main text for definition).

Our results indicate that the fuel break was not sufficient at stopping the wildfire spread. This is not surprising because fire suppression personnel with the required equipment were not able to utilize the fuel break for suppression activities. However, the fuel break did clearly change wildfire behavior by reducing the intensity of the flames, thus reducing the level of burn severity and preserving vegetation health. The postfire observations indicate that the fuel break region contained trees that were still intact with green crown canopies, whereas the surrounding untreated region was severely damaged with no preservation of tree canopies, leaving only the stumps and bare trunks. In-situ measurements quantified the PCV of char, which declined at a rate of approximately 2% per 3 m into the fuel break, with an average of 80% PCV of char dominating the outside of the fuel break, with only 40% within the fuel break (Fig. 4). Aerial drone measurements used to compute GLI, though not robust, indicated an increase in the chlorophyll levels within the fuel break in comparison to outside, suggesting an increase in healthy vegetation within the fuel break. S2 observations found that the burn severity, quantified by dNBR was 5 × less within the fuel break. Furthermore, the vegetation health, as determined by the postfire NDVI was approximately 3 × greater within the fuel break. When comparing postfire NDVI to prefire NDVI, the vegetation health within the fuel break was approximately 1 × less than the prefire, but 5 × less outside the fuel break (Fig. 6). Overall, the fuel treatment was effective at reducing the burn severity, thereby preserving the health of the trees within the fuel break (Fig. 7).

Continued monitoring of fuel breaks in addition to utilizing a combination of multi-scale observations (in-situ, aerial, and spaceborne) is deemed advantageous in improving our understanding of what types of fuel treatment plans are beneficial in the future. Long-term monitoring, spanning five years or more, is crucial for detecting regrowth (Wilkin et al., 2017) and providing valuable insights to guide land management decisions and practices.

5. Availability of data and materials

The datasets used and/or analysed during the current study are available from the corresponding author upon reasonable request.

CRediT authorship contribution statement

Janine A. Baijnath-Rodino: Conceptualization, Data curation, Formal analysis, Investigation, Methodology, Project administration, Resources, Software, Validation, Visualization, Writing – original draft, Writing – review & editing. **Alexandre Martinez:** Formal analysis, Investigation, Methodology, Resources, Software, Validation, Visualization. **Robert A. York:** Conceptualization, Formal analysis, Investigation, Methodology, Resources, Software, Visualization, Writing – original draft, Writing – review & editing. **Efi Foufoula-Georgiou:** Formal analysis, Investigation, Methodology, Project administration, Resources, Validation, Writing – original draft, Writing – review & editing. **Amir AghaKouchak:** Project administration, Resources, Software, Validation, Visualization. **Tirtha Banerjee:** Conceptualization, Data curation, Formal analysis, Investigation, Methodology, Project administration, Resources, Software, Validation, Visualization, Writing – original draft, Writing – review & editing.

Declaration of Competing Interest

The authors declare that they have no known competing financial interests or personal relationships that could have appeared to influence the work reported in this paper.

Data availability

Data will be made available on request.

Acknowledgements

Baijnath-Rodino and Banerjee acknowledge the funding support from the University of California Office of the President (UCOP) grant LFR-20- 653572 (UC Lab-Fees). Banerjee also acknowledges the National Science Foundation (NSF) grants NSF-AGS-PDM-2146520 (CAREER), NSF-OISE-2114740 (AccelNet) and NSF-CPS-2209695; the United States Department of Agriculture (USDA) grant 2021-67022-35908 (NIFA); and a cost reimbursable agreement with the USDA Forest Service 20-CR-11242306-072. Foufoula-Georgiou acknowledges the support by the National Science Foundation (grants DMS-1839336 and ECCS-1839441), NASA's Global Precipitation Measurement program (grant 80NSSC22K0597), and the Center for Ecosystem Climate Solutions (CECS), funded by California Strategic Growth Council's Climate Change Research Program.

References

Agee, J.K., Bahro, B.B., Finney, M.A., Omi, P.N., Sapsis, D.B., Skinner, C.N., van Wagtendonk, J.W., Weatherspoon, C.P., 2000. The use of shaded fuel breaks in landscape fire manage-ment. For. Ecol. Manage. 127, 55–66.

Agee, J.K., Lolley, M.R., 2006. Thinning and prescribed fire effects on fuels and potential fire behavior in and eastern cascades forest, Washington, USA. Fire Ecology 2 (2), 3–19.

Agee, J.K., 1996. The influence of forest structure on fire behavior. In: Proceedings of 17th Forest Vegetation Management Conference. Redding, CA, pp. 52±68.

Banerjee, T., 2020. Impacts of forest thinning on wildland fire behavior. Forests 11 (9), 918.

Banerjee, T., Heilman, W., Goodrick, S., Hiers, J.K., Linn, R., 2020. Effects of canopy midstory management and fuel moisture on wildfire behavior. Sci. Rep. 10 (1), 1–14.

Bright, B.C., Loudermilk, E.L., Pokswinksi, S.M., Hudak, A.T., O'Brien, J.J., 2016. Introducing close–range photogrammetry for characterizing forest understory plant diversity and surface fuel structure at fine scales. Can. J. Remote Sens. 42, 460–472.

Bush, E.R., Mitchard, E.T.A., Silva, T.S.F., Dimoto, E., Dimbonda, P., Makaga, L., Abernethy, K., 2020. Monitoring mega-crown leaf turnover from space. Remote Sens. 12, 429. https://doi.org/10.3390/rs12030429.

Chianucci, F., Disperati, L., Guzzi, D., Bianchini, D., Nardino, V., Lastri, C., Rindinella, A., Corona, P., 2016. Estimation of canopy attributes in beech forests using true colour digital images from a small fixed-wing UAV. Int. J. Appl. Earth Obs. Geoinf. 47, 60–68.

Chu, T., Guo, X., 2013. Remote sensing techniques in monitoring post-fire effects and patterns of forest recovery in boreal forest regions: a review. Remote Sens. (Basel) 6 (1), 470–520.

Cumming, J.A., 1964. Effectiveness of prescribed burning in reducing wildfire damage during periods of abnormally high fire danger. J. For. 62, 535–537.

Dainelli, R., Toscano, P., Di Gennaro, S.F., Matese, A., 2021. Recent advances in unmanned aerial vehicle forest remote sensing—a systematic review. Part I: A General Framework. Forests 12, 327. https://doi.org/10.3390/f12030327.

Eng, L.S., Ismail, R., Hashim, W., Baharum, A., 2019. The use of VARI, GLI, and vigreen formulas in detecting vegetation in aerial images. Int. J. Tech. 10 (7), 1385–1394.

Fassnacht, F.E., Schmidt-Riese, E., Kattenborn, T., Hernández, J., 2021. Explaining sentinel 2-based dNBR and RdNBR variability with reference data from the bird's eye (UAS) perspective. Int. J. Appl. Earth Observ. Geoinform. 1569–8432 https://doi.org/10.1016/j.jag.2020.102262.

Finney, M.A., McHugh, C.W., Grenfell, I.C., 2005. Stand- and landscape-level effects of pre-scribed burning on two Arizona wildfires. Can. J. For. Res. 35, 1714–1722.

Gómez, C., Alejandro, P., Hermosilla, T., Montes, F., Pascual, C., Ruiz, L.Á., Álvarez-Taboada, F., Tanase, M.A., Valbuena, R., 2019. Remote sensing for the Spanish forests in the 21st century: a review of advances, needs, and opportunities. For. Syst. 28, 1–33.

Google Earth Engine (MacOS)_V7: https://code.earthengine.google.com/633f56f31038a8c54d3faf91799f6b93 Source information: https://un-spider.org/advisory-support/recommended- practices/recommended-practice-burn-severity/burn-severity-earth-engine [Accessed December 2022].

Government of California, California State Geoportal: Shape file for Creek Fire Perimeter: https://gis.data.ca.gov/maps/CALFIRE-Forestry::california-fire-perimeters-all/about [Accessed November 2021].

Guimarães, N., Pádua, L., Marques, P., Silva, N., Peres, E., Sousa, J.J., 2020. Forestry remote sensing from unmanned aerial vehicles: a review focusing on the data, processing and potentialities. Remote Sens. 12, 1046.

Hudak, Andrew T.; Rickert, Ian; Morgan, Penelope; Strand, Eva; Lewis, Sarah A.; Robichaud, Peter R.; Hoffman, Chad; Holden, Zachary A. 2011. Review of fuel treatment effectiveness in forests and rangelands and a case study from the 2007 megafires in central, Idaho, USA. Gen. Tech. Rep. RMRS-GTR-252 Fort Collins, CO: U.S. Department of Agriculture, Forest Service, Rocky Mountain Research Station. 60 p.

Ingalsbee T.200. Fuelbreaks for wildland fire management: a moat or a drawbridge for ecosystem fire restoration? Fire Ecology 1, 85–99. doi:10.4996/Fire Ecology .0101085.

Keeley, J.E., 2009. Fire intensity, fire severity and burn severity: a brief review and suggested usage. Int. J. Wildland Fire 18 (1), 116–126.

Keifer, M., van Wagtendonk, J.W., Buhler, M., 2006. Long-term surface fuel accumulation in burned and unburned mixed-conifer forests of the central and southern Sierra Nevada, CA (USA). Fire Ecology 2 (1), 53–72.

Keyes, C.R., O'Hara, K.L., 2002. Quantifying stand targets for silvicultural prevention of crown fires. West. J. Appl. For. 17 (2), 101–109.

Knapp, E.E., Keeley, J.E., Ballenger, E.A., Brennan, T.J., 2005. Fuel reduction and coarse woody debris dynamics with early and late season prescribed fire in a Sierra Nevada mixed conifer forest. For. Ecol. Manage. 208, 383–397.

Louhaichi, M., Borman, M.M., Johnson, D.E., 2001. Spatially located platform and aerial photography for documentation of grazing impacts on wheat. Geocarto Int. 16 (1), 65–70.

Martinson, J., and P.N. Omi. 2003. Performance of fuel treatments subjected to wildfires. Pages 7-13 in: P.N. Omi and L.A. Joyce, technical editors. Fire, fuel treatments, and ecological res-toration. USDA Forest Service Proceedings RMRS-P-29.

Moghaddas, J.J., Craggs, L., 2007. A fuel treatment reduces fire severity and increases sup-pression efficiency in a mixed conifer forest. Int. J. Wildland Fire 16, 673–678.

Moran, C.J., Seielstad, C.A., Cunningham, M.R., Hoff, V., Parsons, R.A., Queen, L., Sauerbrey, K., Wallace, T., 2019. Deriving fire behavior metrics from UAS imagery. Fire 2, 36. https://doi.org/10.3390/fire2020036.

National Wildfire Coordinating Group: Accessed January 2022: https://www.nwcg.gov/term/glossary/fuel-break.

Omi, P.N., Kalabokidis, K.D., 1991. Fire damage on extensively versus intensively managed forest stands within the North Fork Fire, 1988. Northwest Sci. 65, 149–157.

Omi, P.N., 1996. The role of fuelbreaks. In: Proceedings of the 17th Forest Vegetation Management Conference. Redding, CA, pp. 89±96.

Peterson, D.L., J.K. Agee, T. Jain, M. Johnson, D. McKenzie, and E. Reinhardt. 2003. Fuels planning, managing forest structure to reduce fire hazard. Proceedings of the 2nd International Wildland Fire Ecology and Fire Management Congress. Association for Fire Ecology, 16-20 November 2003, Orlando, Florida, USA.

Pollet, J., Omi, P.N., 2002. Effect of thinning and prescribed burning on crown fire severity in ponderosa pine forests. Int. J. Wildland Fire 11, 1–10.

Natural Resource Canada: Accessed June 2022: https://www.nrcan.gc.ca/maps-tools-and-publications/satellite-imagery-and-air-photos/tutorial-fundamentals-remote-sensing/microwave-remote-sensing/airborne-versus-spaceborne-radars/9397.

Richard, B., Yusuke, K., Reily, G., Jessica, B., Bethany, M., Clifford, T.J., Brad, Q., Justin, E., Terry, H., David, G., 2020. Monetising the savings of remotely sensed data and information in burn area emergency response (BAER) wildfire assessment. Int. J. Wildland Fire 30, 18–29. https://doi.org/10.1071/WF19209.

Ritchie, M.W., Skinner, C.N., Hamilton, T.A., 2007. Probability of tree survival after wildfire in an interior pine forest of northern California: effects of thinning and prescribed fire. For. Ecol. Manage. 247, 200–208.

Rouse, J.W., Haas, R.H., Schelle, J.A., Deering, D.W., Harlan, J.C., 1974. Monitoring the vernal advancement of retrogradation of natural vegetation. MD, NASA/GSFC, Type III, Final report, Green-belt, p. 371.

Schmidt, D.A., Taylor, A.H., Skinner, C.N., 2008. The influence of fuels treatment and land-scape arrangement on simulated fire behavior, southern Cascade Range, California. For. Ecol. Manag. 255 (8–9), 3170–3184.

Schoennagel T, Nelson CR, Theobald DM, Carnwath GC, Chapman TB. 2009. Implementation of National Fire Plan treatments near the wildland–urban interface in the western United States. Proceedings of the National Academy of Sciences of the United States of America 106, 10706–10711. doi:10.1073/PNAS.0900991106.

Scott, J.H., and E.D. Reinhardt. 2001. Assessing crown fire potential by linking models of sur-face and crown fire behavior. USDA Forest Service Research Paper RMRS-RP-29.

Shin, P., Sankey, T., Moore, M.M., Thode, A.E., 2018. Evaluating unmanned aerial vehicle images for estimating forest canopy fuels in a ponderosa pine stand. Remote Sens. 10, 1266.

Somvanshi, S.S., Kumari, M., 2020. Comparative analysis of different vegetation indices with respect to atmospheric particulate pollution using sentinel data. Appl. Computing Geosci. 7.

Stephens, S.L., 1998. Evaluation of the effects of silvicultural and fuels treatments on potential fire behaviour in Sierra Nevada mixed-conifer forests. For. Ecol. Manage. 105, 21–35.

Stephens, S.L., Moghaddas, J.J., 2005. Experimental fuel treatment impacts on forest struc-ture, potential fire behavior, and predicted tree mortality in a California mixed conifer forest. For. Ecol. Manage. 215, 21–36.

Stephens, S.L., Moghaddas, J.J., Edminster, C., Fiedler, C.E., Haase, S., Harrington, M., Keeley, J.E., Knapp, E.E., McIver, J.D., Metlen, K., Skinner, C.N., Youngblood, A., 2009. Fire treatment effects on vegetation structure, fuels, and potential fire severity in western US forests. Ecol. Appl. 19 (2), 305–320.

Surovỳ, P., Kuželka, K., 2019. Acquisition of forest attributes for decision support at the forest enterprise level using remote-sensing techniques—a review. Forests 10, 273.

Syphard, A.D., Keeley, J.E., Brennan, T.J. 2011. Factors affecting fuel break effectiveness in the control of large fires on the Los Padres National Forest, International Journal of Wildland Fire, 10, 1071/WF10065.

Syphard, A.D., Scheller, R.M., Ward, B.C., Spencer, W.D., Strittholt, J.R., 2011. Simulating landscape-scale effects of fuels treatments in the Sierra Nevada, California, USA. Int. J. Wildland Fire 20, 364–383.

Vaillant, N.M., Fites-Kaufman, J., Stephens, S.L., 2009. Effectiveness of prescribed fire as a fuel treatment in Californian coniferous forests. Int. J. Wildland Fire 18, 165–172.

van Gerrevink, M.J., Veraverbeke, S., 2021. Evaluating the hyperspectral sensitivity of the differenced normalized burn ratio for assessing fire severity. Remote Sens. (Basel) 13 (22), 1–16. https://doi.org/10.3390/rs13224611 [4611].

Van Wagner, C.E., 1968. The line intercept method in forest fuel sampling. For. Sci. 14, 20–26.

van Wagtendonk, J.W., 1996. Use of a deterministic fire growth model to test fuel treatments. In: Erman, D.C. (Ed.), Sierra Nevada ecosystems project, final report to congress, vol. II. Assessments and Scientific Basis for Management Options. University of California, Davis, pp. 1155–1166. Centers for Water and Wildland Resources Report 37.

VanWagner, C.E., 1977. Conditions for the start and spread of crown fire. Can. J. For. Res. 7, 23–34.

Wagle, R.F., Eakle, T.W., 1979. A controlled burn reduces the impact of a subsequent wildfire in a ponderosa pine vegetation type. For. Sci. 25, 123–129.

Wilkin, K.M., Ponisio, L.C., Fry, D.L., et al., 2017. Decade-long plant community responses to shrubland fuel hazard reduction. fire ecol 13, 105–136. https://doi.org/10.4996/fireecology.130210513.

Yang, D., Meng, R., Morrison, B.D., McMahon, A., Hantson, W., Hayes, D.J., Breen, A.L., Salmon, V.G., Serbin, S.P., 2020. A multi-sensor unoccupied aerial system improves characterization of vegetation composition and canopy properties in the arctic tundra. Remote Sens. 12, 2638. https://doi.org/10.3390/rs12162638.